Electronic Supplementary Material (ESI) for CrystEngComm.
This journal is © The Royal Society of Chemistry 2017

Electronic Supplementary Information

$K_2Mn^{II}_2(H_2O)_2C_2O_4(HPO_3)_2$: A New 2D Manganese(II) Oxalatophosphite with Double-Layered Honeycomb Sheets Stabilized by Potassium Ions

Joseba Orive,[a,] Ramesh Sivasamy,[a] Roberto Fernández de Luis,[b,c] Edgar Mosquera,[d] and María I. Arriortua[b,c]*

[a] Departamento de Ciencia de los Materiales, FCFM, Universidad de Chile, Av. Beauchef 851, Santiago 8370448, Chile.

[b] Departamento de Mineralogía y Petrología, Facultad de Ciencia y Tecnología, Universidad del País Vasco (UPV/EHU), Apdo. 644, 48080 Bilbao, Spain.

[c] Basque Center for Materials, Applications & Nanostructures (BC Materials) Parque Tecnológico de Zamudio, Camino de Ibaizabal, Edificio 500 - 1º, 48160 Derio, Spain.

[d] Departamento de Física, Universidad del Valle, A.A. 25360, Cali, Colombia.

* Corresponding author:
joseba.orive@ing.uchile.cl
Phone: +56 229784237. Fax: +56 226994119

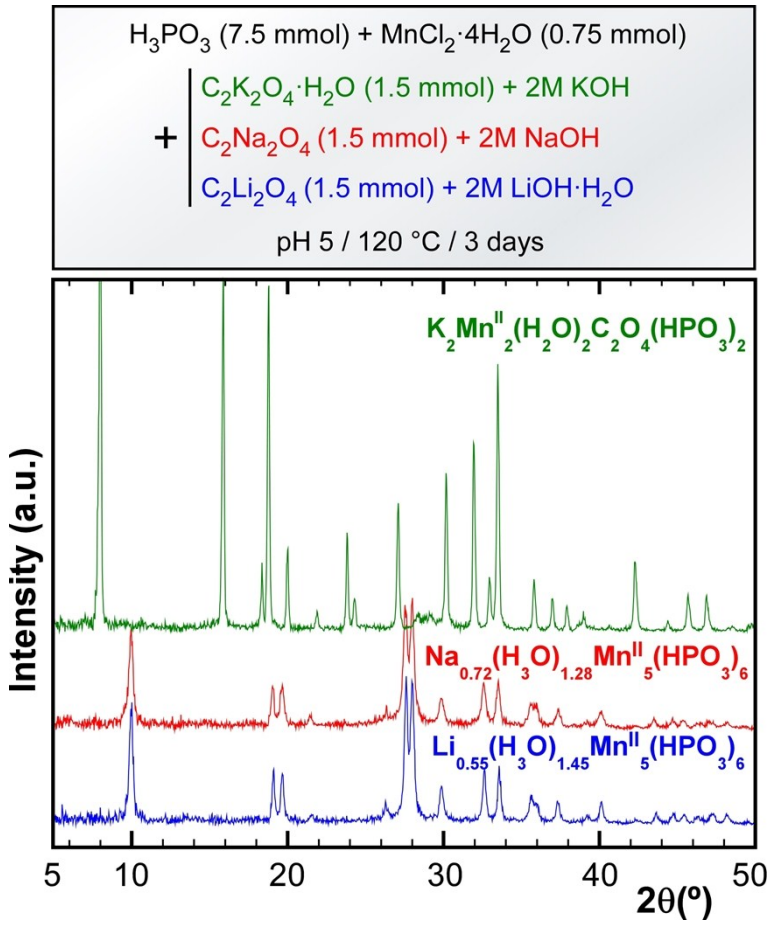

Figure S1. X-ray diffraction patterns of the phosphites obtained depending on the alkali metal hydroxide and oxalate in the hydrothermal synthesis.

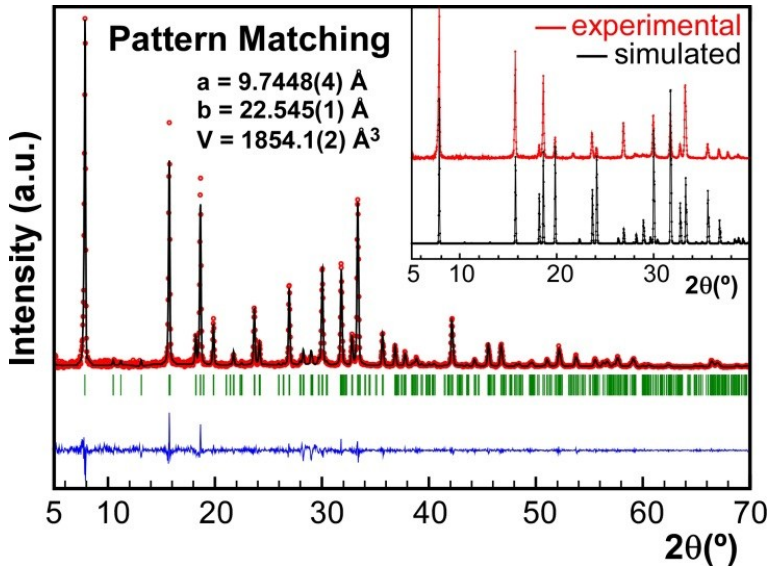

Figure S2. Observed (red dots), calculated (black line) and difference powder X-ray diffraction pattern (blue line) for the pattern matching analysis of **KMnCP**. Inset shows the comparison between the simulated and experimental powder X-ray diffraction patterns.

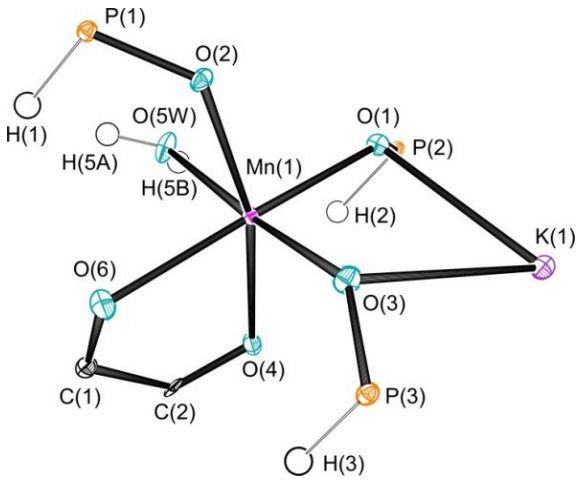

Figure S3. Asymmetric unit of $K_2Mn_2(H_2O)_2C_2O_4(HPO_3)_2$ with displacement parameters drawn at the 50% probability level.

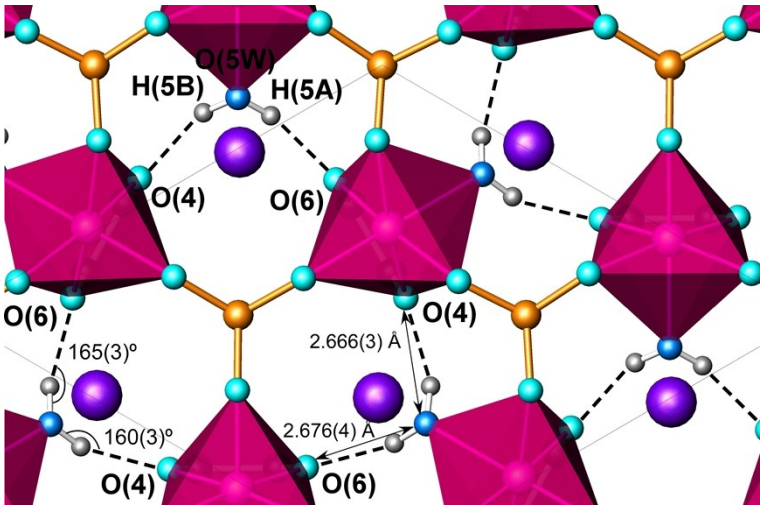

Figure S4. Intralayer hydrogen bonds scheme of **KMnCP**.

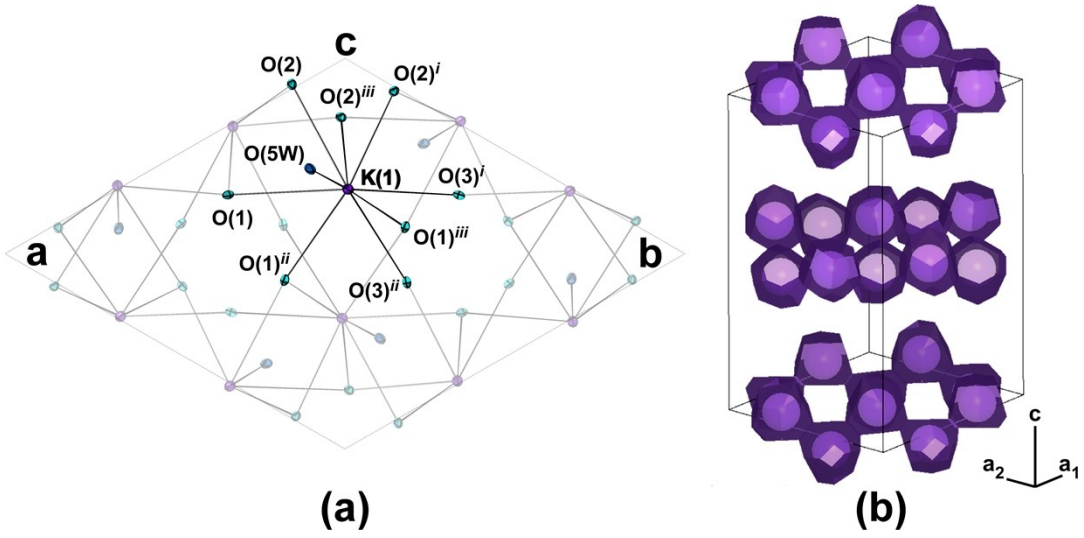

Figure S5. (a) Coordination environment of K(1) atoms. **(b)** *VDP* representation of the K^+ ions located in the interlayer spaces of **KMnCP**.

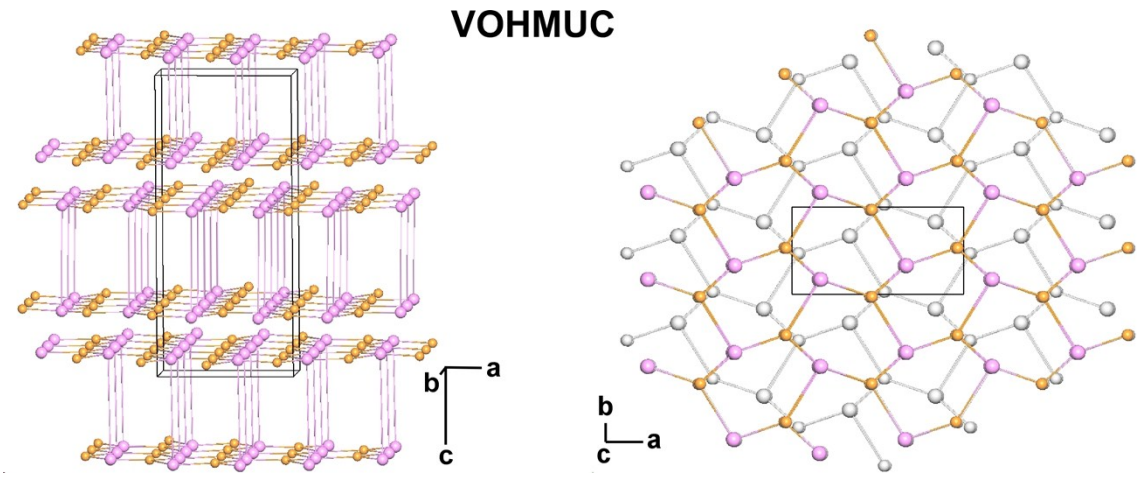

Figure S6. Topological representation of the not interpenetrated 3,4L147 topology previously reported, VOHMUC.

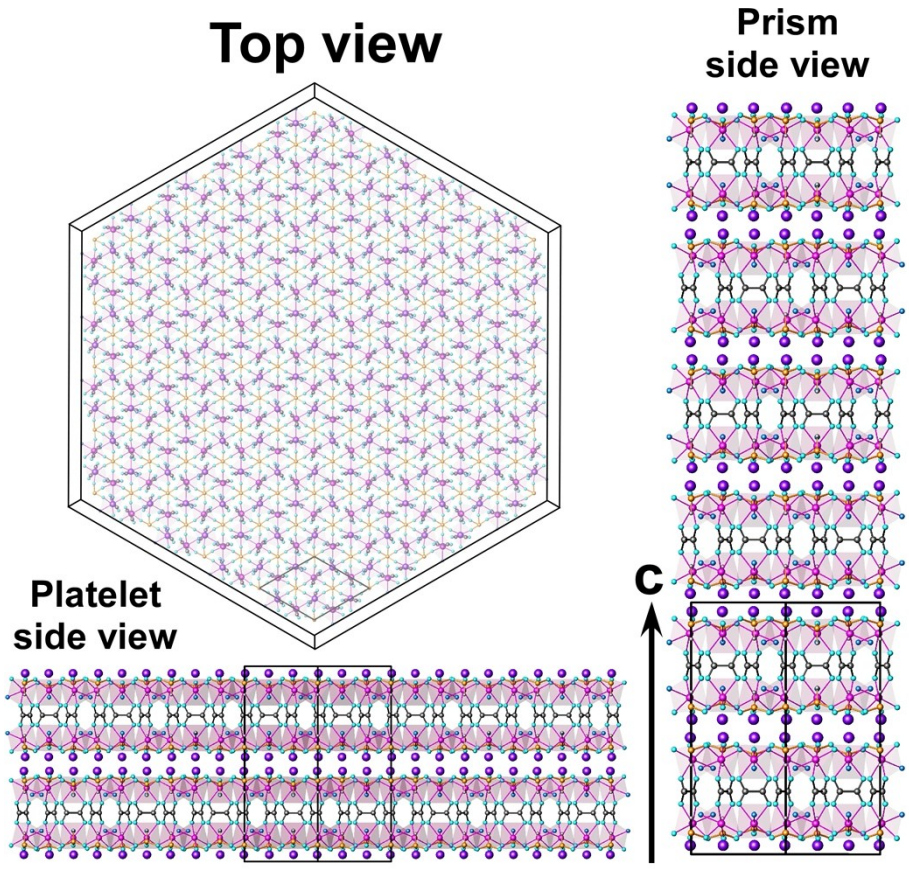

Figure S7. Crystallographic model showing the top view of a hexagonal plate and the growth of the **KMnCP** structure in the ab plane and c directions.

0D and 1D metal oxalatophosphites

$(C_4N_2H_{12})_3[In_2(HPO_3)_2(C_2O_4)_4]\cdot 4H_2O$ Class. **MP_0O_0** Ref [5c]

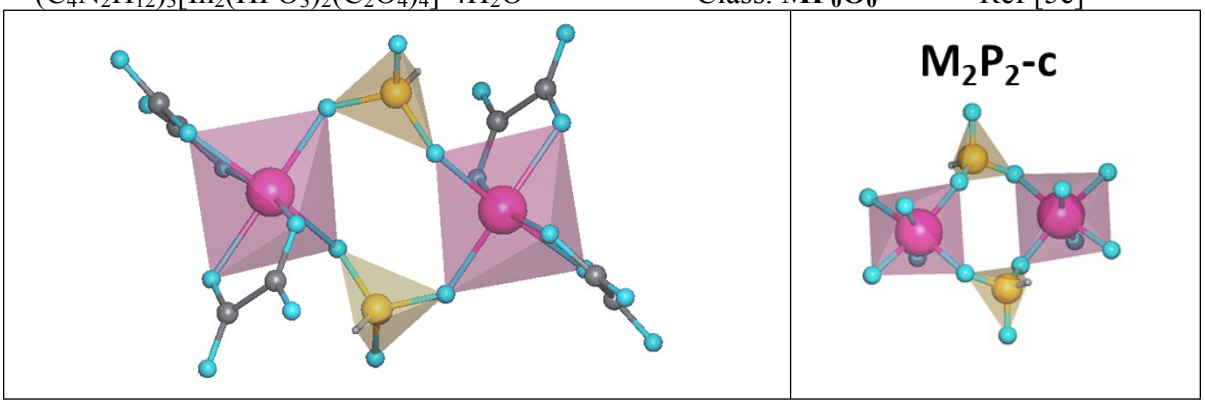

$(C_6N_2H_{14})_2[Ga_2(OH)_2(C_2O_4)_2(HPO_3)_2]\cdot 2H_2O$ Class. **MP_1O_1** Ref [9c]

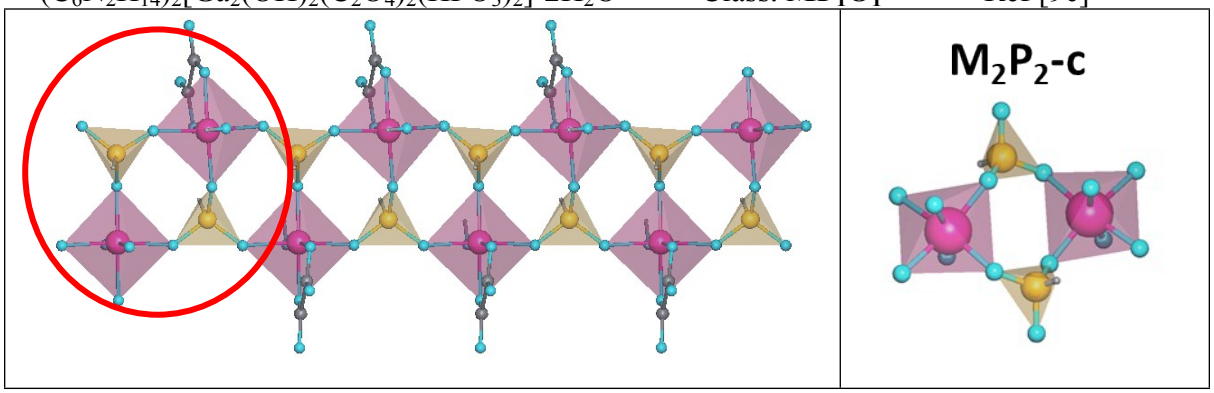

$(C_6N_2H_{14})_2[Fe^{III}_2F_2(HPO_3)_2(C_2O_4)_2]\cdot 2H_2O$ Class. **MP_1O_1** Ref [8a]

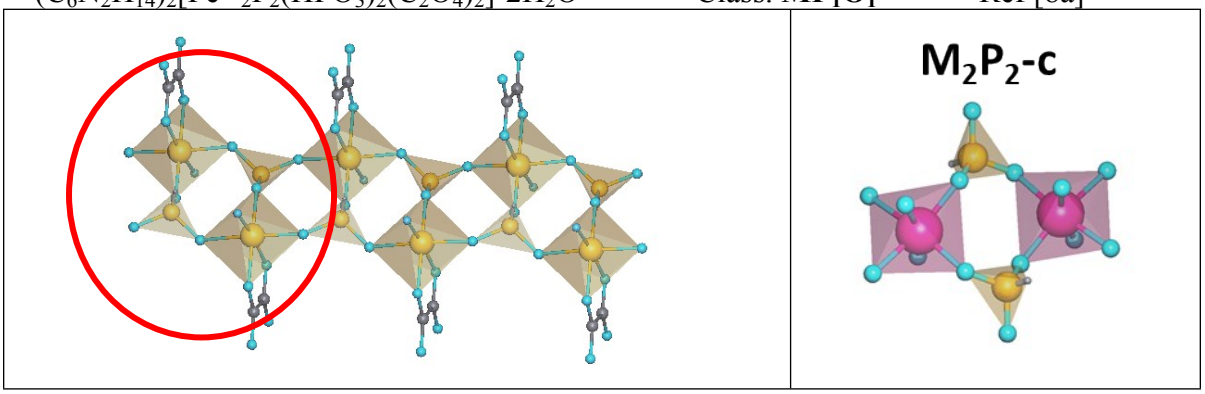

Continue on next page…

2D metal oxalatophosphites

$(C_6N_4H_{21})_2[Fe^{II}_4(HPO_3)_2(C_2O_4)_5]\cdot 5H_2O$ Class. **MP_0O_2** Ref [8a]

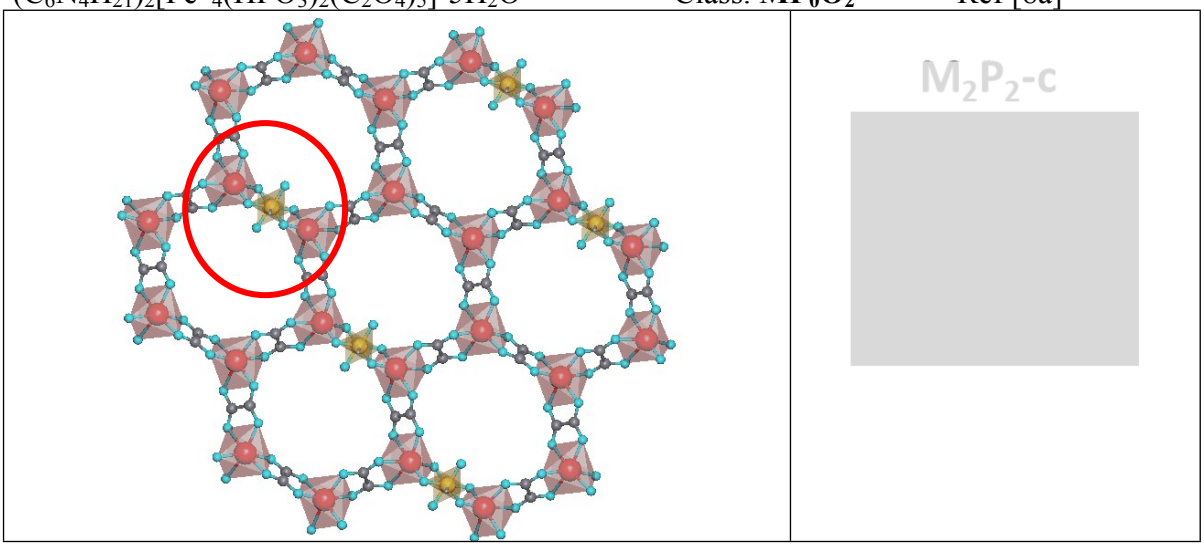

$A_2[(VO)_2(HPO_3)_2(C_2O_4)]\cdot nH_2O$ (A=Li, Na, K, NH_4) and
$C_6N_2H_{18})_{0.5}[Ga(OH)(C_2O_4)_{0.5}(HPO_3)]$ Class. **MP_1O_2** Ref [12a, b] [9c]

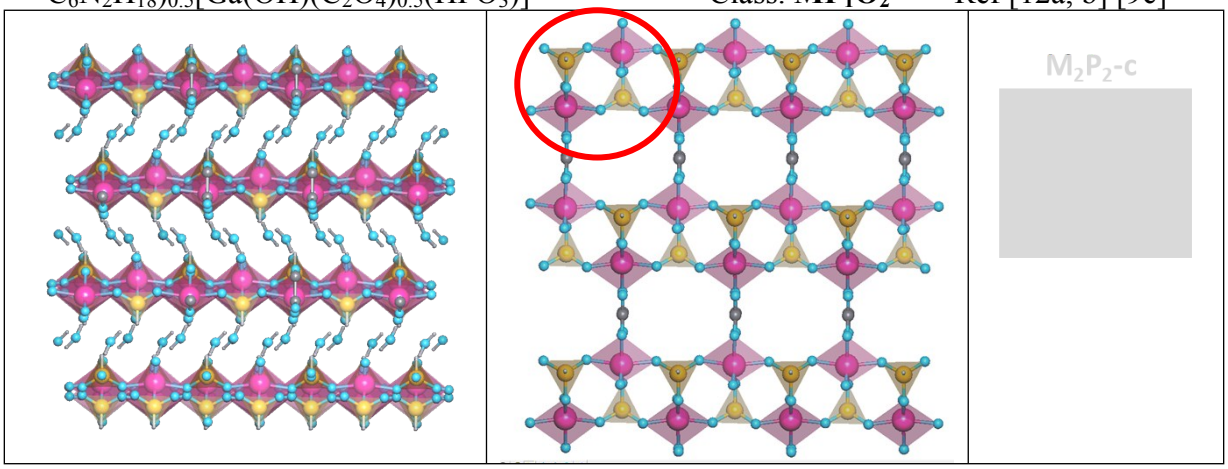

$(C_6N_2H_{16})[Ga_2(HPO_3)_2(H_2PO_3)_2(C_2O_4)]$ and
$[H_2apm][Ga_2(HPO_3)_2(H_2PO_3)_2(C_2O_4)]$ Class. **MP_1O_2** Ref [9a, b]

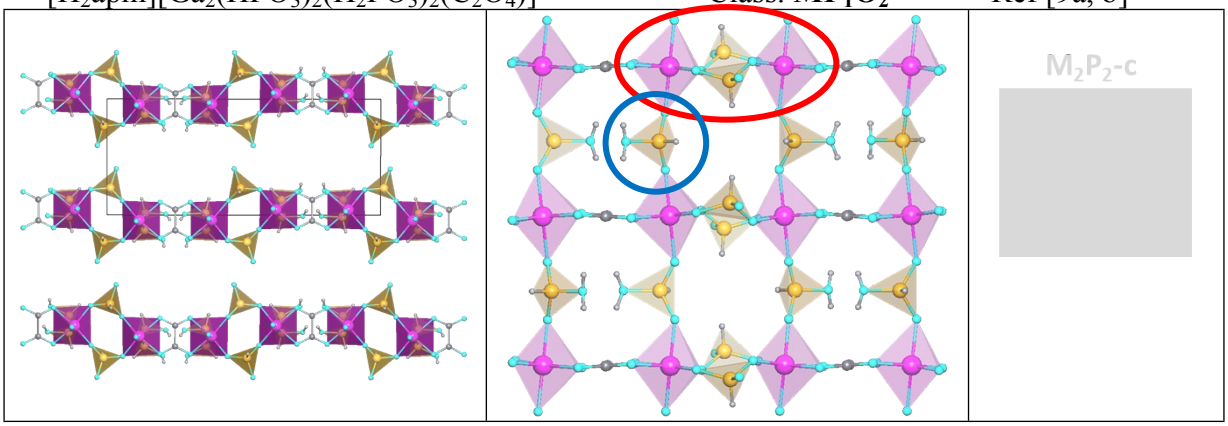

Continue on next page…

2D metal oxalatophosphites

$(C_4N_2H_{12})_2[In_2(HPO_3)_3(C_2O_4)_2]\cdot 3H_2O$ Class. **MP_2O_2** Ref [5c]

Stacking view
2D single layers

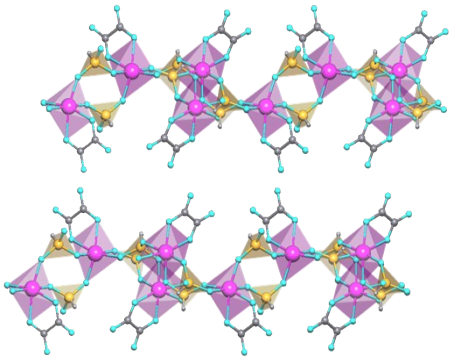

Top layer view

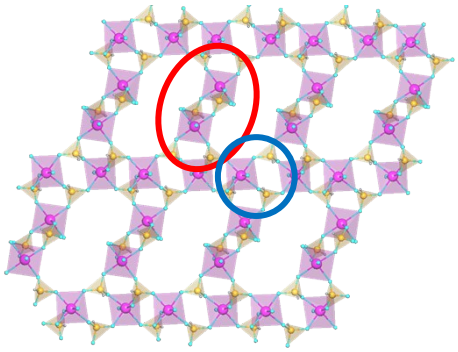

M_2P_2-c

M_1P_2

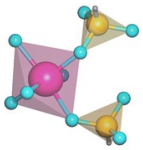

$(C_4N_2H_{12})_3[In_4(HPO_3)_6(C_2O_4)_3]$ Class. **MP_2O_2** Ref [5c]

Stacking view
2D double layers

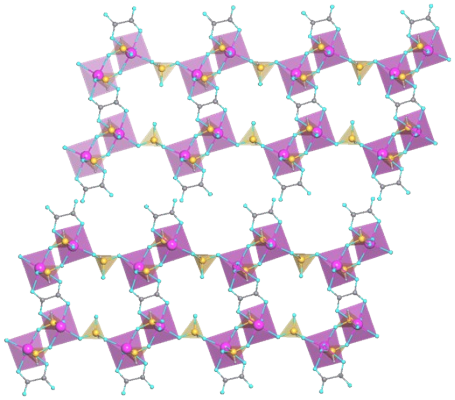

Top layer view

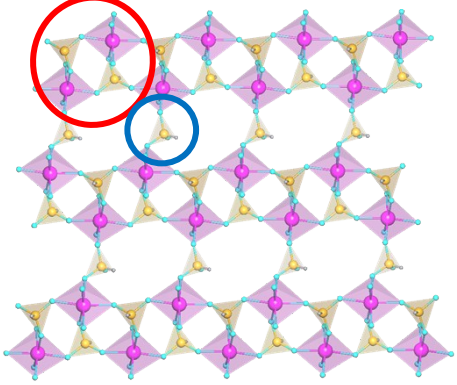

M_2P_2-c

$K_2[Mn^{II}_2(H_2O)_2C_2O_4(HPO_3)_2]$ Class. **MP_2O_2** Ref [This work]

Stacking view
2D double layers

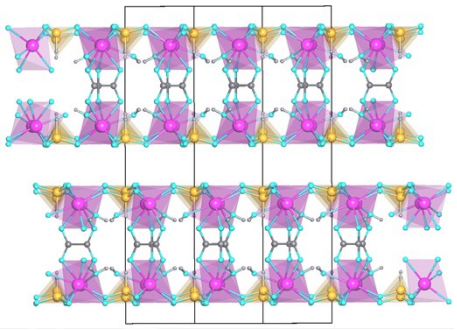

Top layer view

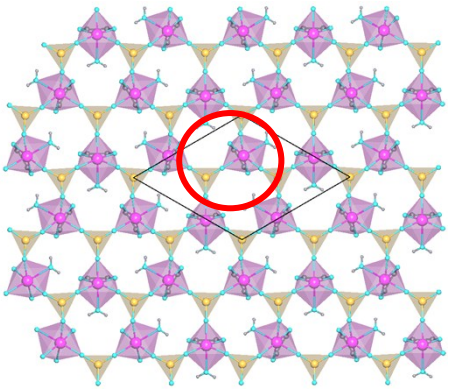

M_1P_1

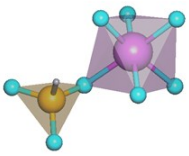

Continue on next page…

3D metal oxalatophosphites

$(C_4N_2H_{12})[M^{II}_4(HPO_3)_2(C_2O_4)_3]$ (M= Fe, Co) and
$(C_5N_2H_{14})[Fe^{II}_4(HPO_3)_2(C_2O_4)_3$ Class. **MP_1O_3** Ref [8a, b] [6a]

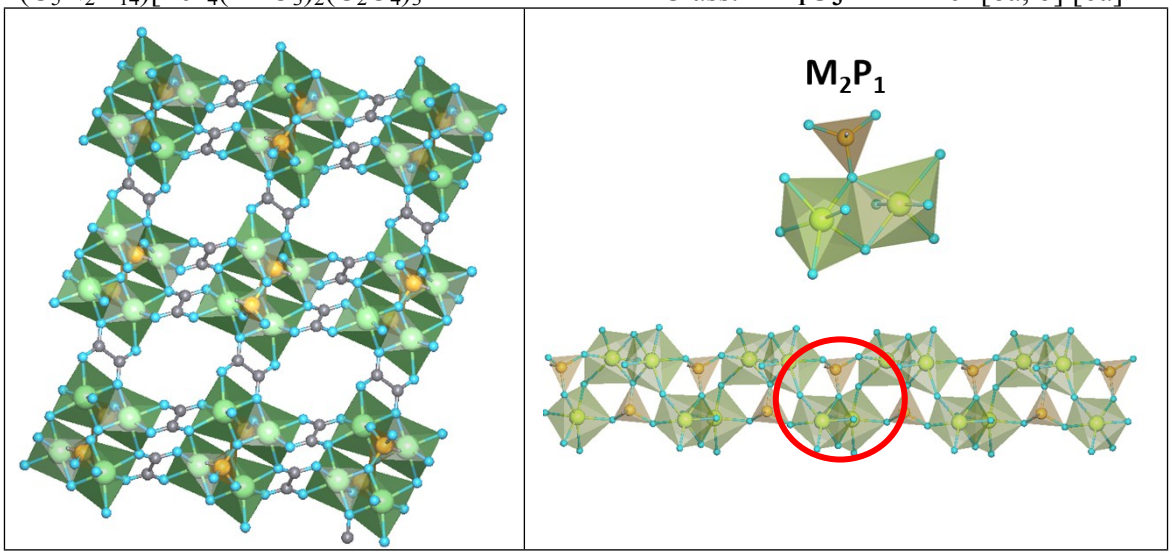

$(CN_3H_6)_2 \cdot Mn_{2.5}(HPO_3)(C_2O_4)_{2.5}(H_2O) \cdot H_2O$ Class. **MP_1O_3** Ref [7a]

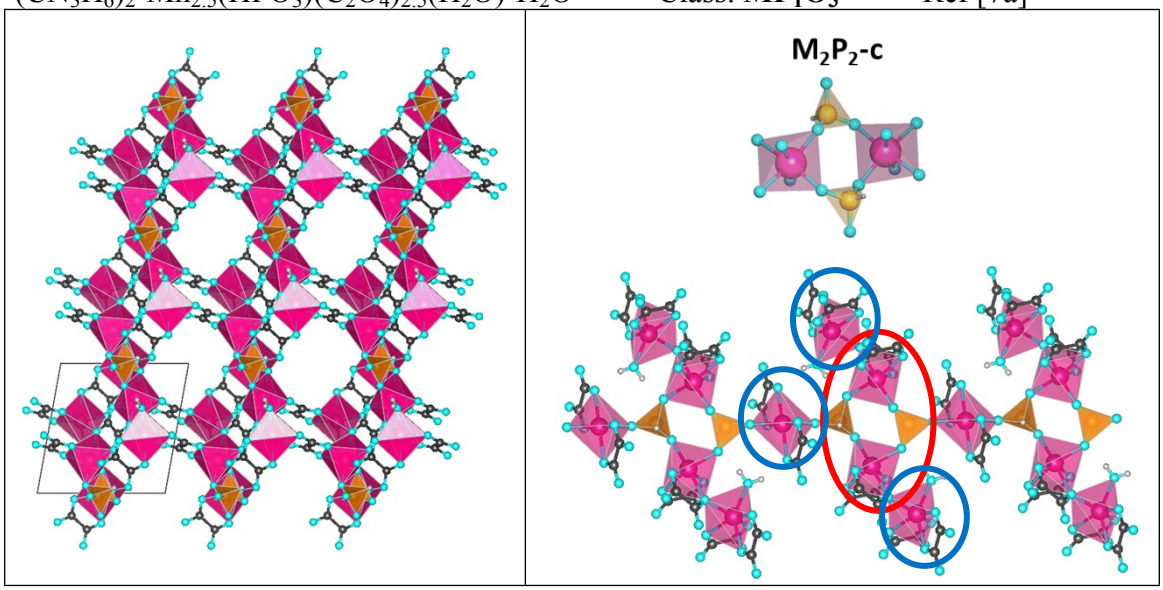

Continue on next page…

3D metal oxalatophosphites

$[C_4N_2H_{12}][In_2(HPO_3)_3(C_2O_4)]$ Class. **MP_2O_3** Ref [5b]

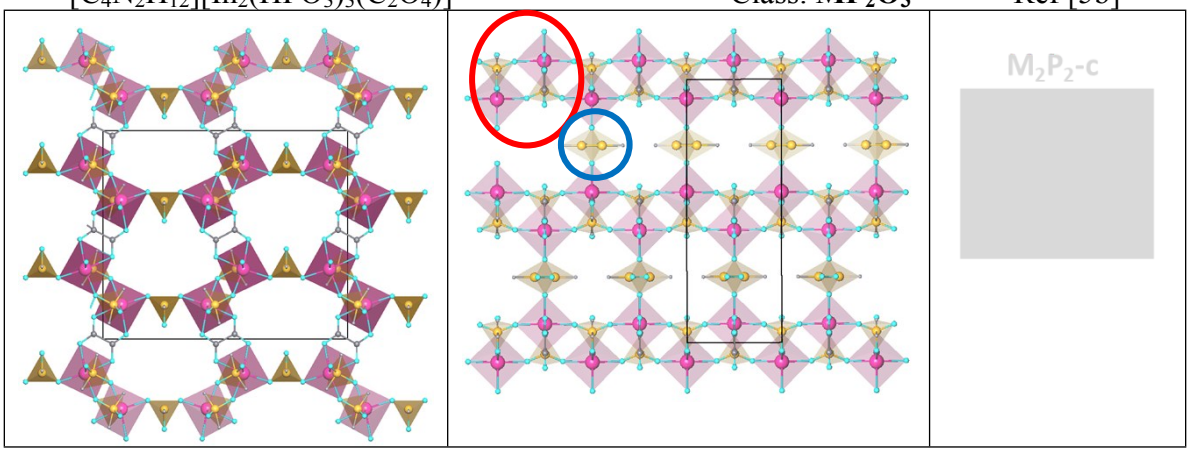

$H[In_5(HPO_3)_6(H_2PO_3)_2(C_2O_4)_2]\cdot(C_4N_2H_{11})_2\cdot H_2O$ Class. **MP_2O_3** Ref [5a]

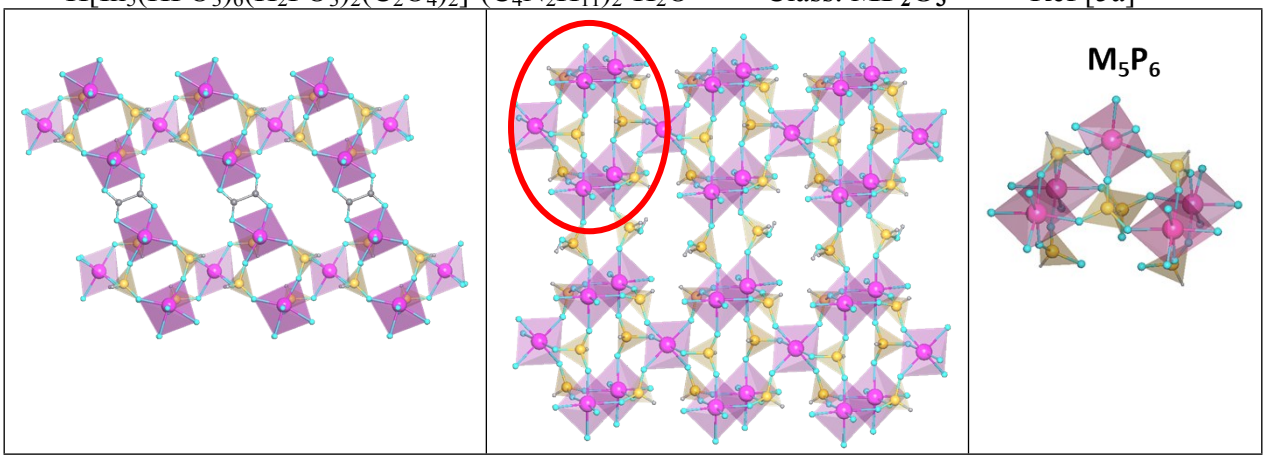

$(C_4N_2H_{12})[Mn^{II}_2(HPO_3)_2(C_2O_4)]$ Class. **MP_2O_3** Ref [7d]

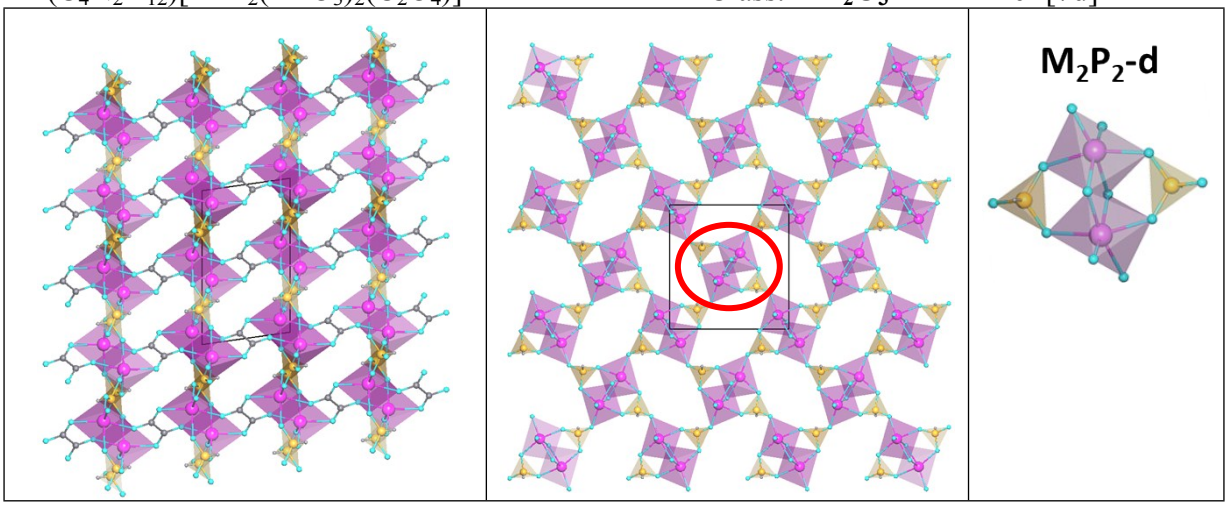

Continue on next page…

3D metal oxalatophosphites

$(C_2N_2H_{10})[M^{II}_2(OH_2)_2(HPO_3)_2(C_2O_4)]$ (M= Mn, Fe) Class. **MP_2O_3** Ref [7c] [8a]

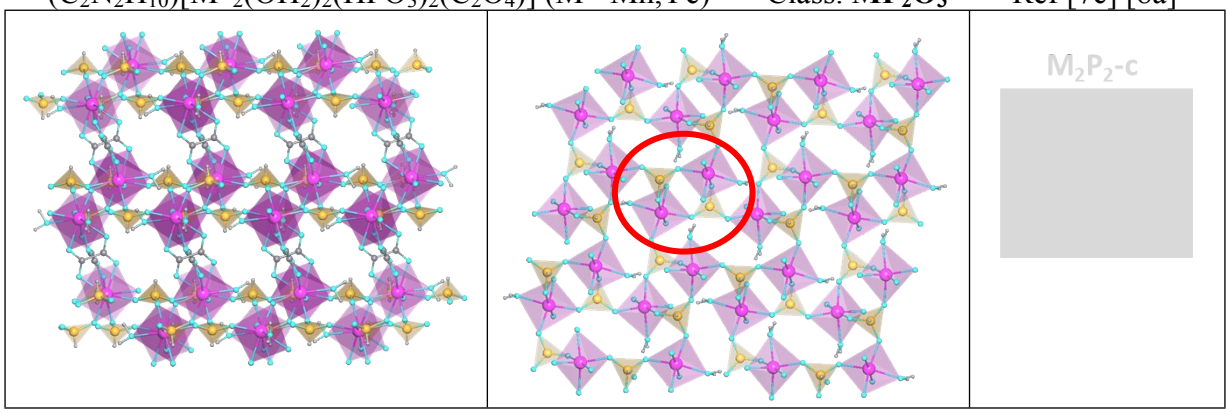

$(H_2dab)[Mn_2(HPO_3)_2(C_2O_4)(H_2O)_2]$ Class. **MP_2O_3** Ref [7b]

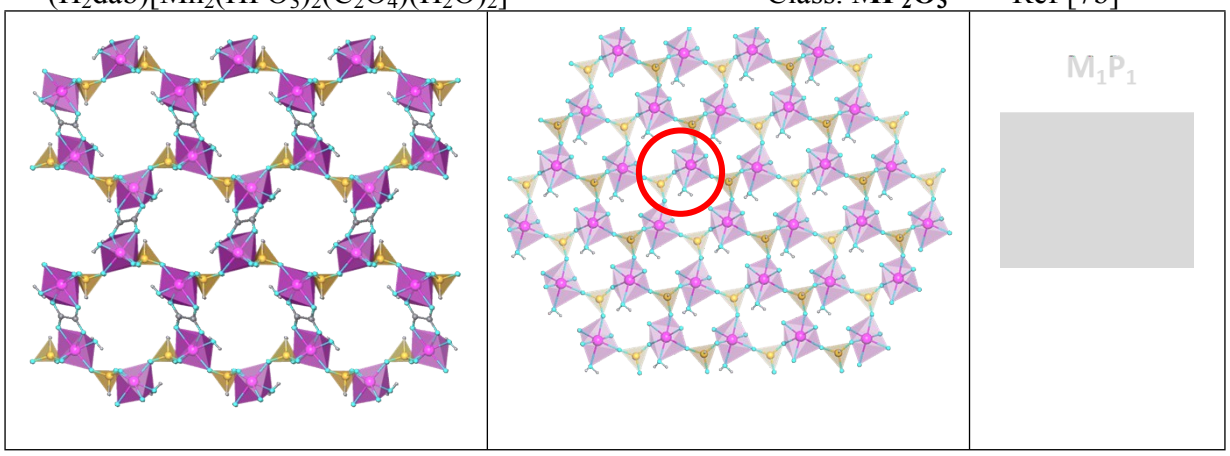

$(C_6N_2H_{16})_{0.5}[Ga_2(HPO_3)_2(H_2PO_3)(C_2O_4)]$ Class. **MP_3O_3** Ref [9b]

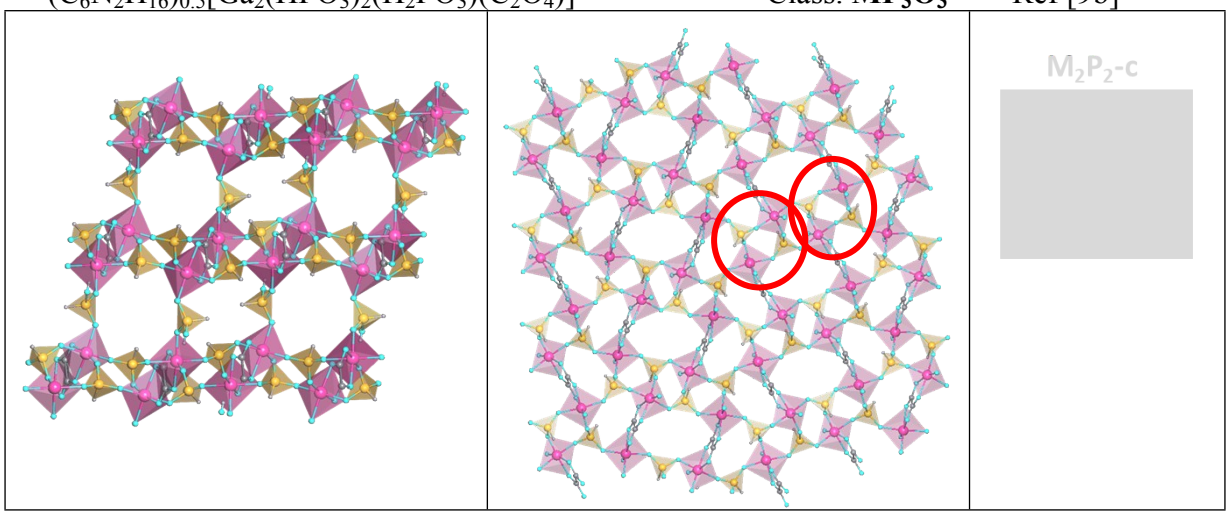

Continue on next page…

3D metal oxalatophosphites

$(C_6H_{14}N_2)[In_2(HPO_3)_3(C_2O_4)]$ Class. **MP_3O_3** Ref [5d]

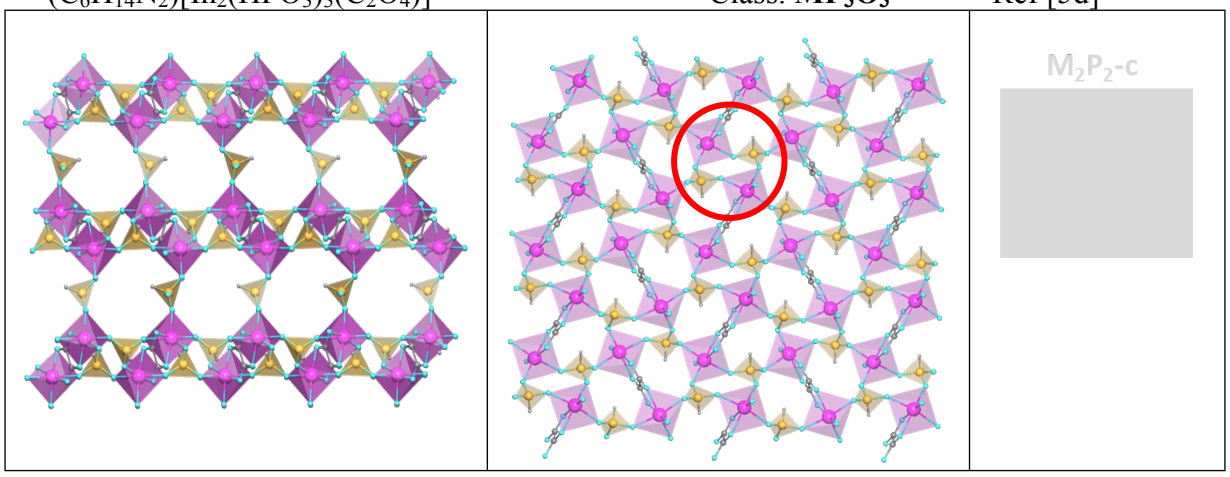

$(C_8N_4H_{26})[Fe^{III}_6(HPO_3)_8(C_2O_4)_3]\cdot 4H_2O$ Class. **MP_3O_3** Ref [8a]

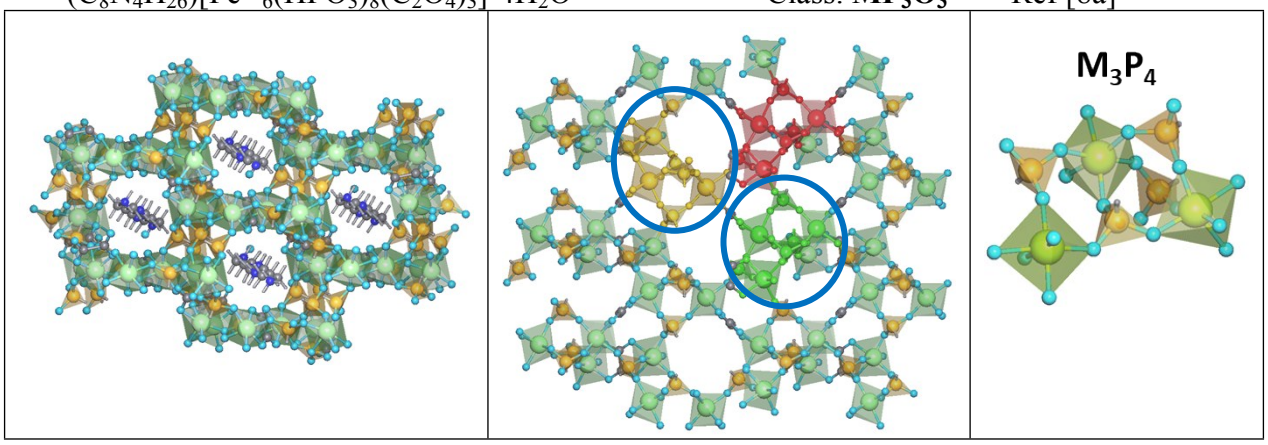

$(C_4N_2H_{14})[In_4(H_2O)(HPO_3)_5(C_2O_4)_2]\cdot 2H_2O$ Class. **MP_3O_3** Ref [5c]

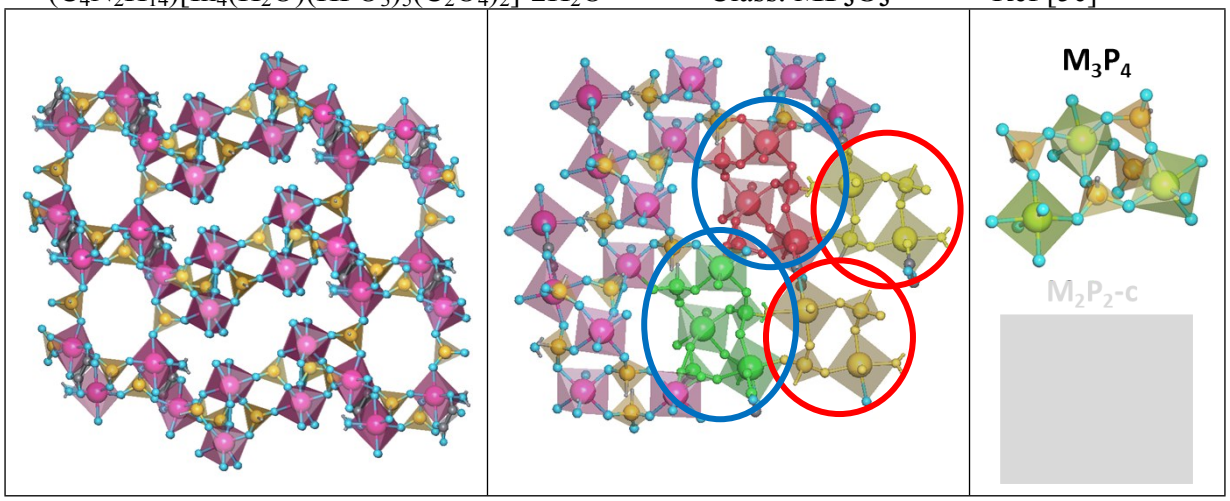

Figure S8. Structural visualization of the analysed metal oxalatophosphites with anionic frameworks. The compounds graphics order follows the same one that observed in Table 2 of the manuscript.

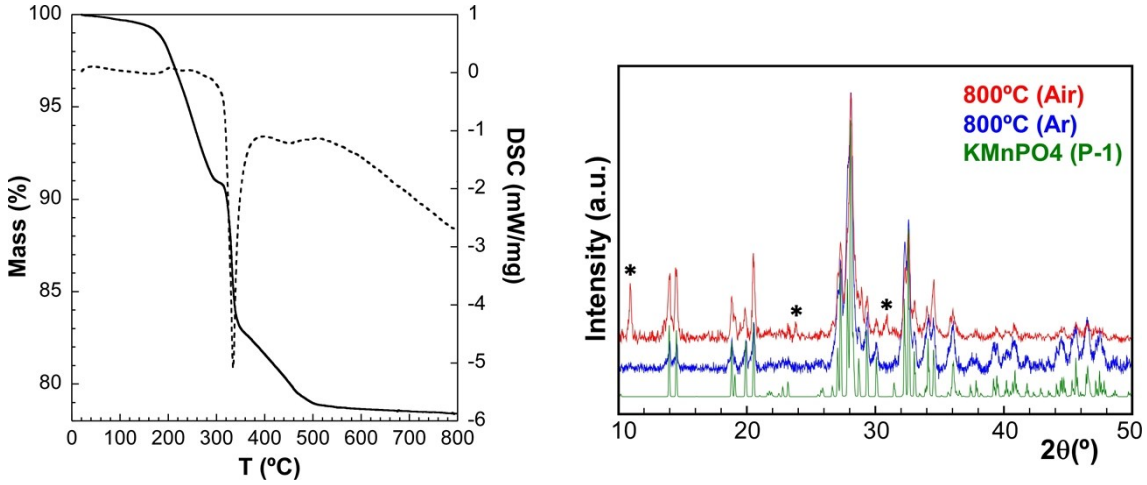

(a) **(b)**

Figure S9. (a) Thermal analysis (TGA, DSC) of **KMnCP**. **(b)** Diffraction patterns of calcination products (red) after TGA analysis in oxygen atmosphere, (blue) after heat treatment in argon atmosphere and (green) simulated pattern for $KMnPO_4$ for comparison. Asterisks represent an unidentified compound.

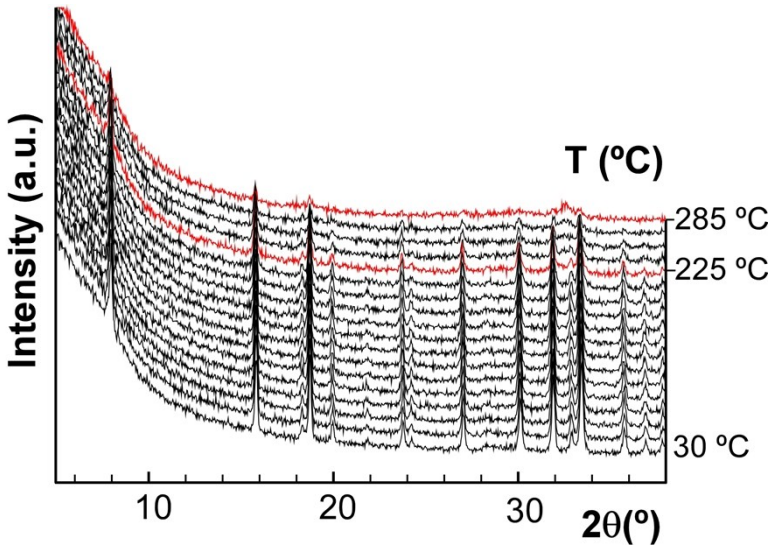

Figure S10. Thermodiffractogram of **KMnCP**.

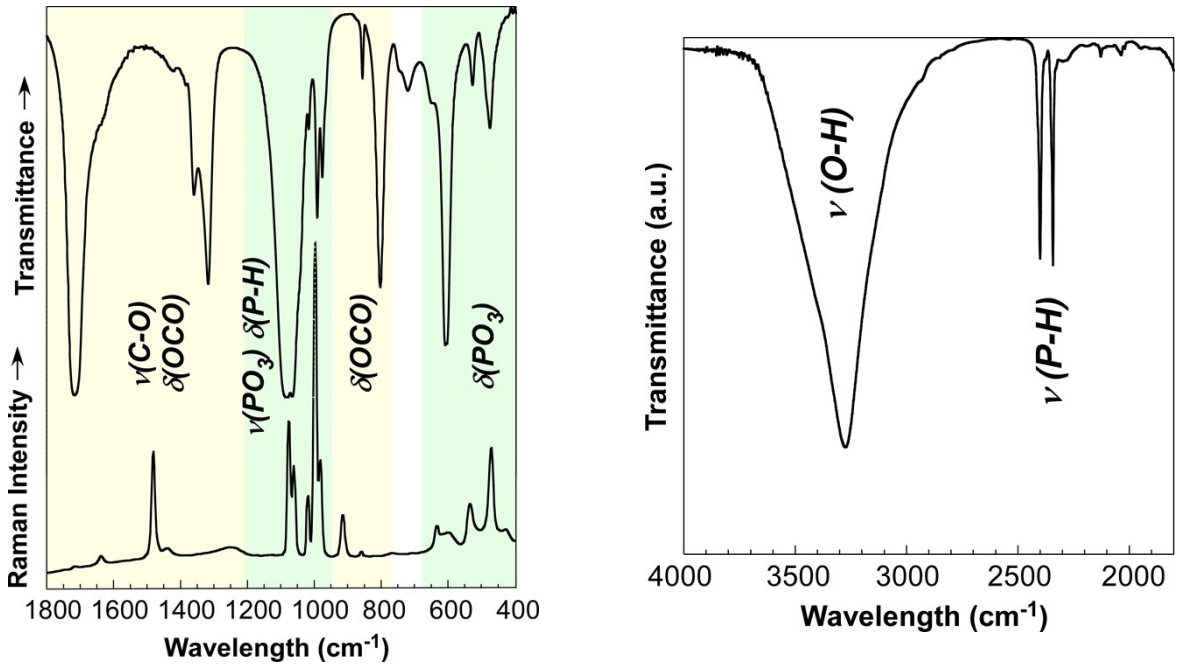

Figure S11. (a) Infrared and Raman spectra comparison of **KMnCP**.
(b) Detail of the ν(P-H) and ν(O-H) vibrational modes of the IR spectrum.

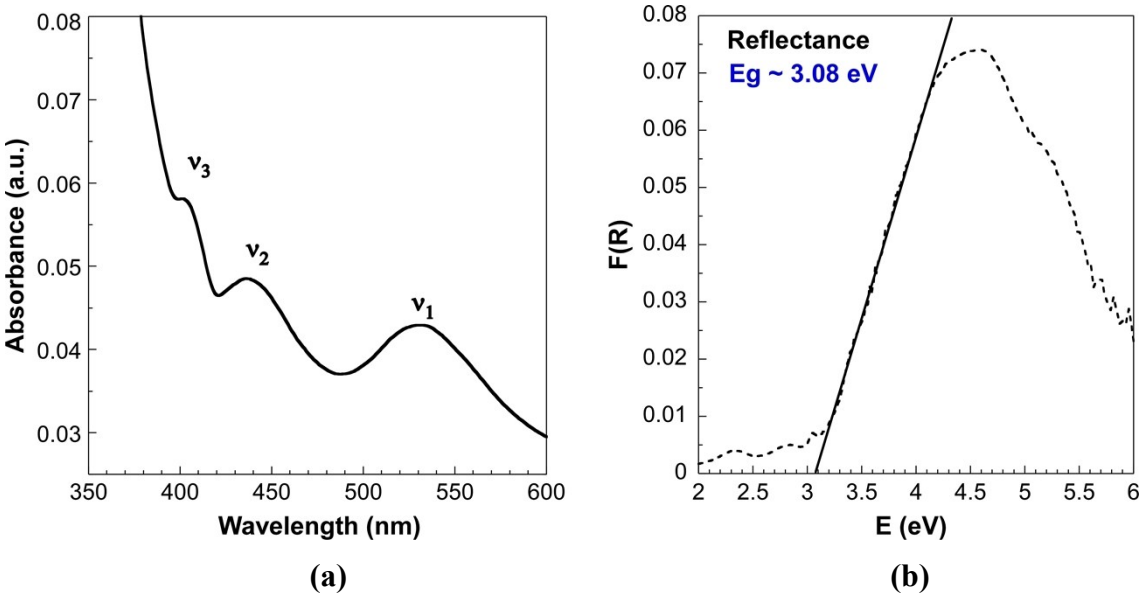

Figure S12. (a) UV-Vis diffuse absorbance spectrum and **(b)** the corresponding F(R) *vs* E (eV) curve of **KMnCP**.

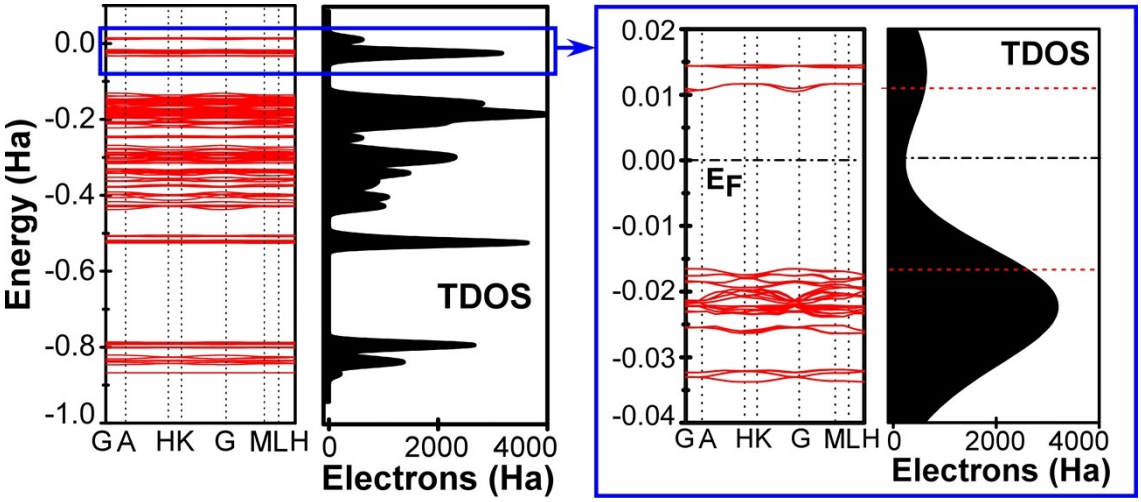

Figure S13. Calculated band structure with total density of states (TDOS) of **KMnCP**. The Fermi level is chosen as the energy reference at 0 eV.

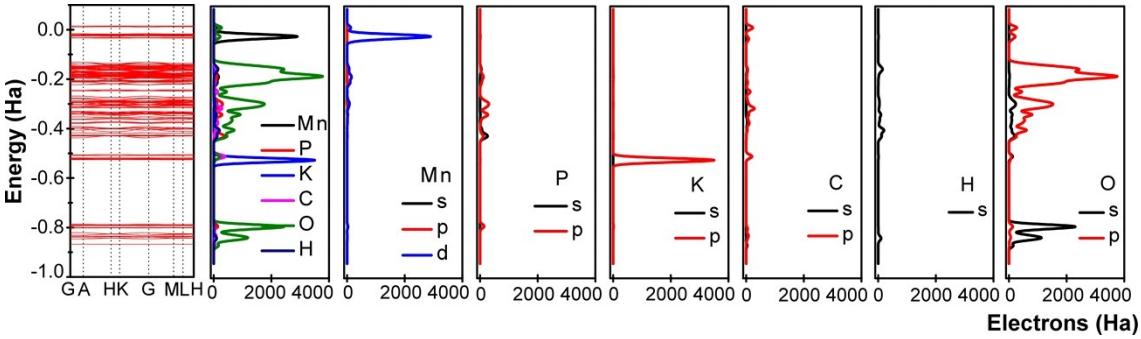

Figure S14. Band structure with partial density of states (PDOS) of **KMnCP**.

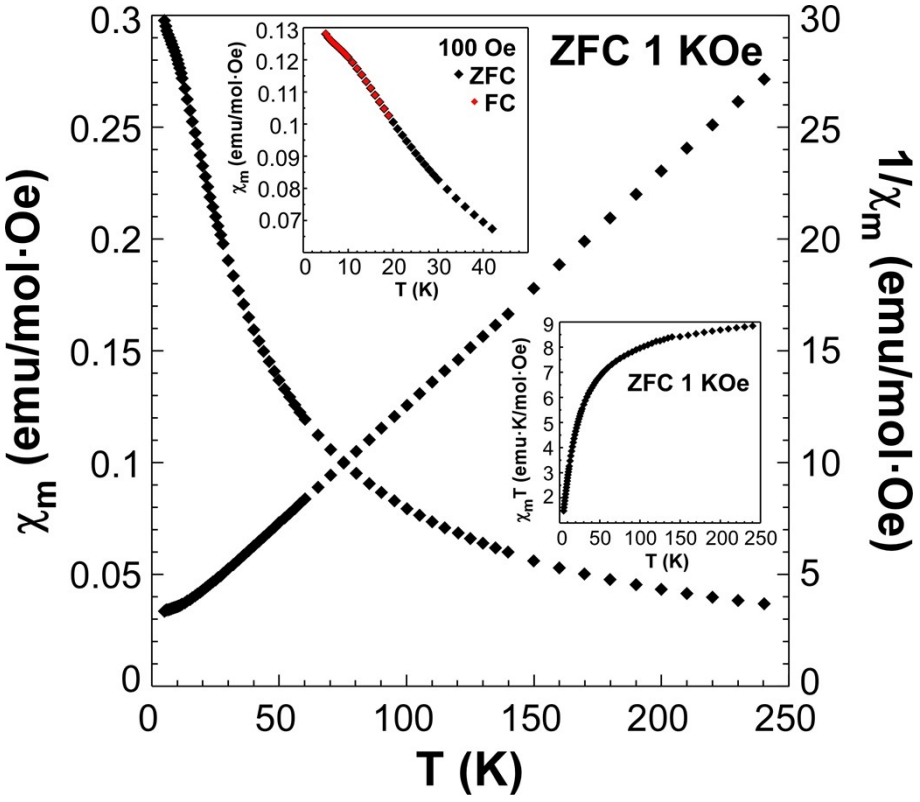

Figure S15. Temperature dependence of χ_m and $1/\chi_m$ for **KMnCP** measured under 1 kOe. The lower inset shows the temperature dependence of $\chi_m T$ and the upper inset an enlargement of the low-temperature region of ZFC–FC data measured under 100 Oe.

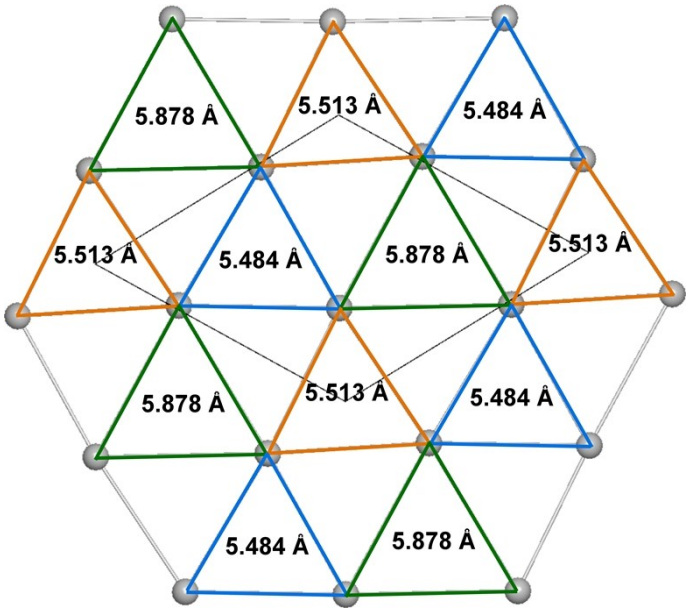

Figure S16. Ideal hexagonal honeycomb Mn(II) layer of **KMnCP** where phosphorous nodes have been suppressed. Mn(II) cations are grouped in triangular clusters with three different values of Mn···Mn intralayer distances.

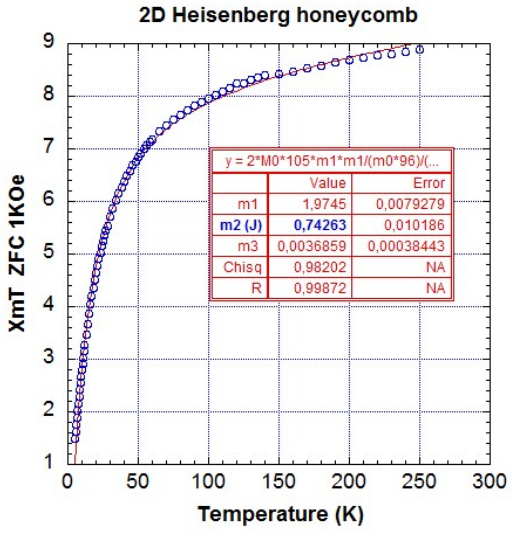

(a)

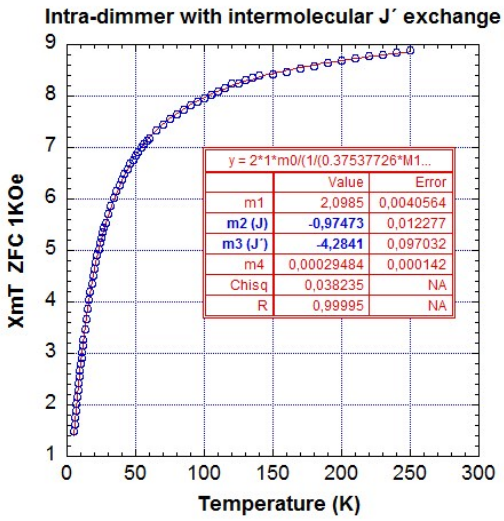

(b)

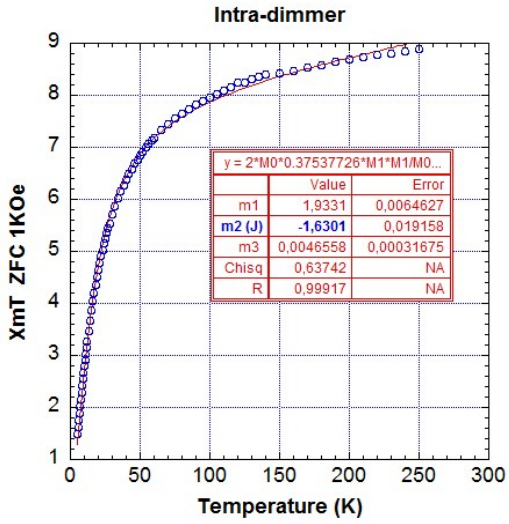

(c)

Figure S17. Magnetic data fitting of **KMnCP**. (a) m1= g, m2= J, m3= χ_m constant; (b) m1=g, m2= J (intra-dimmer), m3= J´ (inter-dimmer), m4= χ_m constant; (c) m1= g, m2 = J (intra-dimmer), m3= χ_m constant.

Hexagonal 2D Heisenberg Mn layer model:

$$\chi_m = \frac{105*g^2}{96*T}(1 - 17.5J/T + 110.833(J/T)^2 + 304.111(J/T)^3 - 999.829(J/T)^4 - 9346.14(J/T)^5 + 264381(J/T)^6)$$

Mn S=5/2 dimmers (Intra-dimmer J) model:

$$\chi_m = 0.37537726g^2 \frac{(55+30e^{-10J/T}+14e^{-18J/T}+30e^{-24J/T}30e^{-28J/T})}{(11+9e^{-10J/T}+7e^{-18J/T}+5e^{-24J/T}+3e^{-28J/T}+e^{-30J/T})}$$

Mn S=5/2 dimmers (Intra-dimmer J + Inter-dimmer J´) model:

$$\chi_m' = N\beta^2 g^2 \frac{\chi_m}{1 - zJ'\chi_m}$$

Table S1. Bond distances (Å) and angles (°) for $K_2Mn^{II}_2(H_2O)_2C_2O_4(HPO_3)_2$.

[Mn(1)O$_6$] octahedron

Mn(1)	O(3)	O(2)	O(1)	O(4)	O(6)	O(5W)
O(5W)	175.92(6)	85.23(7)	85.84(7)	83.63(6)	84.45(6)	***2.245(1)***
O(6)	98.87(7)	93.92(6)	166.05(6)	73.41(5)	***2.237(2)***	
O(4)	99.55(7)	163.85(6)	95.58(6)	***2.227(2)***		
O(1)	91.29(7)	95.23(5)	***2.161(2)***			
O(2)	92.16(6)	***2.139(2)***				
O(3)	***2.125(1)***					

[K(1)O$_9$] polyhedron

K(1)	(O2)^{iii}	(O1)^{i}	(O1)	(O2)^{i}	(O5W)^{ii}	(O3)	(O3)^{iii}	(O2)^{ii}	(O1)^{ii}
(O1)^{ii}	112.97(5)	129.82(4)	51.27(5)	97.67(5)	60.19(4)	111.93(4)	146.47(5)	62.96(8)	***3.042(2)***
(O2)^{ii}	51.48(6)	134.55(6)	112.56(5)	68.14(6)	59.51(5)	145.35(5)	112.75(4)	***3.041(2)***	
(O3)^{iii}	64.62(4)	78.57(5)	113.40(4)	111.72(5)	88.32(4)	50.83(5)	***2.954(2)***		
(O3)	113.49(5)	76.86(5)	64.04(4)	142.90(5)	87.58(4)	***2.946(2)***			
(O5W)^{ii}	75.40(5)	163.85(4)	75.72(5)	127.64(5)	***2.940(2)***				
(O2)^{i}	71.62(7)	66.91(4)	129.24(5)	***2.935(2)***					
(O1)	151.10(4)	100.73(5)	***2.830(2)***						
(O1)^{i}	106.71(5)	***2.824(2)***							
(O2)^{iii}	***2.785(2)***								

[HP(1)O$_3$] pseudotetrahedron

P(1)	(O2)^{xi}	(O2)^{x}	(O2)	H(1)
H(1)	106.00(7)	106.00(7)	106.00(7)	***1.32(5)***
(O2)	112.71(6)	112.70(6)	***1.526(2)***	
(O2)^{x}	112.71(6)	***1.526(2)***		
(O2)^{xi}	***1.526(2)***			

Oxalate [C$_2$O$_4$]

C(1)-C(2)	1.554(4)
C(1)-O(6)	1.252(2)
C(2)-O(4)	1.250(2)
O(6)-C(1)-O(6)^{xii}	126.9(3)
O(6)-C(1)-C(2)	116.6(2)
O(4)-C(2)-O(4)^{xii}	127.4(3)
O(4)-C(2)-C(1)	116.3(2)

[HP(2)O$_3$] pseudotetrahedron

P(2)	(O1)^{ii}	(O1)	(O1)^{vii}	H(2)
H(2)	106.13(7)	106.13(7)	106.13(7)	***1.33(4)***
(O1)^{vii}	112.59(6)	112.59(6)	***1.531(1)***	
(O1)	112.59(6)	***1.531(1)***		
(O1)^{ii}	***1.531(2)***			

[HP(3)O$_3$] pseudotetrahedron

P(3)	(O3)^{v}	(O3)^{iii}	(O3)	H(3)
H(3)	106.78(7)	106.78(7)	106.78(7)	***1.30(4)***
(O3)	112.03(6)	112.03(6)	***1.527(1)***	
(O3)^{iii}	112.03(6)	***1.527(1)***		
(O3)^{v}	***1.527(1)***			

Symmetry codes: *i* = -x+1, -y+1, -z+2; *ii* = -y+1, x-y+1, z; *iii* = -x+y+1, -x+1, z; *iv* = x-1, y-1, z; *v* = -y+1, x-y, z; *vi* = y, -x+y+1, -z+2; *vii* = -x+y, -x+1, z; *viii* = x-y+1, x, -z+2; *ix* = x+1, y+1, z; *x* = -y, x-y, z; *xi* = -x+y, -x, z; *xii* = x, y, -z+3/2

Table S2. Assignment of the vibrational spectra of **KMnCP** (band positions in cm^{-1})

Assignment	**IR**	**Raman**
ν(O-H)	3275 (vs)	-----
ν(P-H)	2344 (m), 2402 (m)	-----
ν_{as}(C-O)	1714 (vs), 1635 (w)	1713 (vw), 1635 (w)
ν_{s}(C-O)	1360 (m), 1318 (s)	1480 (m), 1440 (w)
$\nu_{as}(PO_3)$	1087 (vs), 1067 (vs)	1075 (m), 1060 (m)
δ(P-H)	1018 (w)	1018 (w)
$\nu_{s}(PO_3)$	992 (m), 978 (m)	996 (s), 981 (m)
δ(OCO)+ν(C-C)	858 (w), 805 (s)	914 (w), 857 (w)
$\rho(H_2O)$	748 (w), 723 (w)	-----
$\delta_{s}(PO_3)$	652 (w), 608 (s)	631 (w), 598 (w)
$\delta_{as}(PO_3)$	530 (w), 480 (m)	532 (w), 470 (m), 428 (w)
ν, stretching; δ, deformation; s, symmetric; as, asymmetric; s, strong; m, medium; w, weak; sh, shoulder; v, very.		